Interconversion between bound and free conformations of LexA orchestrates the bacterial SOS response

Matej Butala[1,*], Daniel Klose[2], Vesna Hodnik[1], Ana Rems[1], Zdravko Podlesek[1], Johann P. Klare[2], Gregor Anderluh[1], Stephen J. W. Busby[3], Heinz-Jürgen Steinhoff[2] and Darja Žgur-Bertok[1]

[1]Department of Biology, Biotechnical Faculty, University of Ljubljana, Večna pot 111, 1000 Ljubljana, Slovenia, [2]Department of Physics, University of Osnabrück, Barbarastrasse 7, D-49076 Osnabrück, Germany and [3]School of Biosciences, University of Birmingham, Birmingham B15 2TT, UK

ABSTRACT

The bacterial SOS response is essential for the maintenance of genomes, and also modulates antibiotic resistance and controls multidrug tolerance in subpopulations of cells known as persisters. In *Escherichia coli*, the SOS system is controlled by the interplay of the dimeric LexA transcriptional repressor with an inducer, the active RecA filament, which forms at sites of DNA damage and activates LexA for self-cleavage. Our aim was to understand how RecA filament formation at any chromosomal location can induce the SOS system, which could explain the mechanism for precise timing of induction of SOS genes. Here, we show that stimulated self-cleavage of the LexA repressor is prevented by binding to specific DNA operator targets. Distance measurements using pulse electron paramagnetic resonance spectroscopy reveal that in unbound LexA, the DNA-binding domains sample different conformations. One of these conformations is captured when LexA is bound to operator targets and this precludes interaction by RecA. Hence, the conformational flexibility of unbound LexA is the key element in establishing a co-ordinated SOS response. We show that, while LexA exhibits diverse dissociation rates from operators, it interacts extremely rapidly with DNA target sites. Modulation of LexA activity changes the occurrence of persister cells in bacterial populations.

INTRODUCTION

In unstressed, growing *Escherichia coli* cells, the SOS system is shut off due to repression by LexA of $\sim$50 promoters that control expression of the SOS regulon (1,2). Under these conditions, *E. coli* is thought to contain $\sim$1300 molecules of LexA (3). Most LexA is DNA bound, but $\sim$20% is thought to be free. LexA is a homodimeric protein (4) that likely locates its target sites by multiple dissociation–reassociation events within the same DNA molecule (5). Around each landing site, the repressor is thought to diffuse along non-specific DNA and to undergo rotation-coupled sliding to facilitate the search for specific binding sites (6).

The majority of *E. coli* SOS promoters are regulated by LexA alone (7). LexA activity is modulated by the active form of RecA (RecA*), that stimulates self-cleavage of a scissile peptide bond between Ala84 and Gly85, thereby de-activating LexA (8), lowering LexA's affinity for the DNA and exposing residues that target LexA for ClpXP and Lon protease degradation (9). As a result, the cellular concentration of LexA drops from $\sim$2 to $\sim$0.2 µM, thereby de-repressing SOS genes (3).

A key characteristic of the SOS response is the orchestrated induction of individual SOS genes. Thus, initially, genes with low-affinity SOS boxes are expressed, enabling protection and maintenance of the structural integrity of the replisome, while genes with high-affinity operators are expressed late in the SOS response (1). To circumvent unrepaired DNA damage, even after high-fidelity nucleotide excision, and recombinational repair, low fidelity DNA damage tolerance pathways are induced, presumably to increase bacterial mutation rates

and survival in times of stress (10). As DNA damage is repaired, LexA accumulates and the system is reset. Alternatively, if cells are severely damaged and may not survive, the sensing of long-lived-inducing signal triggers the synthesis of bacteriocins and prophages, resulting in cell lysis (11). Thus, RecA* also catalyzes self-cleavage of lambdoid phage repressors (12) whose catalytic, carboxy-terminal domains (CTDs) exhibit homology with the LexA CTD (13).

Similarly to LexA inactivation, cleavage of phage repressors leads to destruction of the protein's abilities to firmly bind DNA, enabling a switch from the latent or lysogenic to replicative and lytic phase. Interestingly, the λ cI repressor is cleaved only when monomeric (14), while the cI repressor of the temperate 434 bacteriophage is inactivated preferably when bound to specific DNA (15). LexA is predominately dimeric in the cell (4) and repressor dimers can undergo RecA*-mediated self-cleavage when off the DNA (16). Therefore, the mechanisms of repressor inactivation among various biological systems related to SOS functions vary from one system to another.

Even though many studies have investigated the SOS response, it is still unclear how diversity within SOS boxes co-ordinates temporal induction of the different SOS genes. In addition, it is not known how RecA* induces self-cleavage of LexA and which are the structural determinants required for RecA*-mediated cleavage of LexA (16,17). Here, we present the first report describing LexA repressor with defects in LexA–RecA* interaction. We demonstrate that, the unbound LexA structure is highly flexible in contrast to the rigid DNA-bound state, in which interaction with RecA* is precluded. Thus, we show that RecA* indirectly activates the SOS system, by mediating a decrease in the intracellular pool of unbound LexA provoking dissociation of the operator-bound repressor and concomitantly inducing the LexA regulon genes. Our data further imply that two sequential interactions of the unbound LexA with RecA* are required for inactivation of both subunits of the LexA repressor dimer.

MATERIALS AND METHODS

Cloning, expression and isolation of the proteins

The *lexA*, *recA* and *oxyR* genes were amplified by polymerase chain reaction (PCR) from the *E. coli* K-12 strain RW118 (18) using oligonucleotide primers LexA_u, LexA_d; RecA_u, RecA_d or OxyR_u, OxyR_d, respectively (Supplementary Table S1). The PCR products were subsequently cut with BamHI and MluI and cloned into an expression vector (19) to prepare plasmids pAna1, pAna2 and pOxyR. The LexA and RecA proteins overexpressed from the pAna1 or pAna2 plasmids, respectively, were constructed as His$_6$ fusion proteins with an N-terminal hexa-histidine tag and a thrombin cleavage site ((H)$_6$SSLVPRGS). A variant of the pAna1 expression plasmids, pLexA29, pLexA54, pLexA71, pLexA119, pLexA71-119 and pLexA191 were constructed employing the QuickChange® Site-directed Mutagenesis kit manual (Stratagene) and pairs of oligonucleotides 29AC_1, 29AC_2 and 54GC_1, 54GC_2; 71EK_1, 71EK_2;

119SA_1, 119SA_2 or 191LC_1, 191LC_2 (Supplementary Tables S1 and S2), respectively. Proteins LexA, LexA29, LexA54, LexA71, LexA119, LexA191 and RecA were expressed with a His-tag present on the N-terminus in the *E. coli* BL21 (DE3) strain and purified from the bacterial cytoplasm by Ni-chelate chromatography and gel-filtration chromatography (20). Purified proteins were stored at −80°C in 20 mM NaH$_2$PO$_4$ (pH 7.3), 200 mM NaCl except for LexA, LexA71 and RecA which were stored in buffer containing 20 mM Tris−HCl (pH 7.3), 200 mM NaCl. Protein concentrations were determined using NanoDrop1000 (Thermo SCIENTIFIC) (4). Three LexA cysteine mutants (LexA29, LexA54, LexA191) were used for the electron paramagnetic resonance (EPR) analysis. The LexA71 repressor variant exhibits enhanced DNA-binding affinity, but the mechanism for the improved DNA binding is unknown (21). The LexA119 is a non-cleavable repressor derivative with modified Ser119 in the active center to Ala; this mutation does not affect the ability of LexA to bind RecA* (13,16). Thus, the LexA119 variant was used to prevent repressor self-cleavage during the study of the LexA−RecA* interaction.

Operator-containing DNA fragments

The 88 bp *recA* and the 114 bp *tisB* operator-containing DNA fragments were PCR amplified. The colicin K encoding plasmid pKCT1 and its derivatives with altered SOS boxes pKCT3-UP1, pKCT3-UP3 (22) were used to amplify the 121 bp *cka*, *cka*-UP1 and the *cka*-UP3 fragment, respectively. Centered on the generated DNA fragments were none, single or double LexA-binding sites presented in Figure 1. One strand of the amplified PCR products was biotinylated at the 5′-end, and primers RecA_1, RecA_2; TisB_1, TisB_2 were used to amplify DNA fragments with *recA* or *tisB* operators and primers Cka_1, Cka_2 to amplify DNA fragments harboring *cka*, *cka*-UP1 and *cka*-UP3 operators, respectively (Supplementary Table S1). The PCR generated fragments were gel purified (QIAquick kit, Qiagen).

LexA repressor cleavage assays

Activation of the RecA filament (10 μM), carried out on ice for 2 h, and the RecA*-induced (2 μM) cleavage of LexA (1.8 μM) at 37°C interacting with specific or non-specific DNA (∼1.5 μM) were performed as described previously for the unbound LexA repressor (16). The LexA dimer to operator/modified operator ratio was 1:2. The LexA repressor was preincubated with specific and non-specific DNA or for the titration reactions with increasing concentrations of DNA for 10 min at 37°C in a DNA-binding buffer (23). The reaction time course was initiated with the addition of the RecA*. The proteolytic cleavage reactions (20 μl) were stopped by adding 4xNuPAGE LDS sample buffer (Invitrogen). Samples were analyzed on 12% NuPAGE gels (Invitrogen) and stained by Page blue protein stain (Fermentas). The experiments were conducted at least three times and representative gels are shown. The resolved bands were quantified using a G:Box (Syngene). The integrated optical
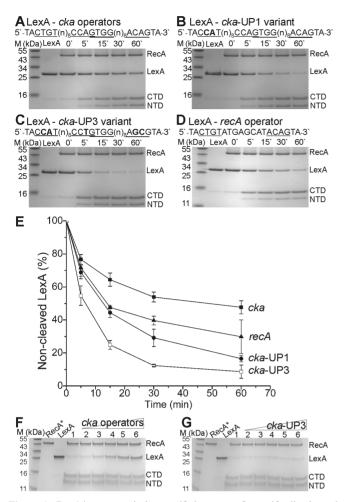
Figure 1. RecA* cannot induce self-cleavage of specifically bound LexA. (**A–D**) Time course (min) of RecA*-induced LexA proteolysis showing inhibition of cleavage due to operator DNAs compared with non-specific DNA (*cka*–UP3). Operator sequences used are presented with SOS boxes underlined and mutated nucleotides in bold typeface. (**E**) Quantitations of the LexA self-cleavage presented are averages with the standard deviation of at least triplicate reactions. (**F**) LexA was pre-incubated with operators or (**G**) non-specific DNA in a ratio 1:0.2; 0.7; 1.2; 1.6; 2.1 (mol:mol) for lanes from 2 to 6, or without DNA for lane 1. The RecA*-activated self-cleavage of LexA was stopped after 15 min. RecA protein, LexA repressor and its cleaved products are marked by the CTD or NTD for the dimerization or the DNA-binding domain, respectively.

density of the intact LexA monomer was normalized to that determined for the RecA protein to account for lane-dependent artifacts. The ratio of LexA cleavage was calculated as the ratio of the normalized density value for the intact LexA relative to the normalized value of LexA exposed to RecA*.

Cross-linking of LexA repressor

Glutaraldehyde cross-linking: at the indicated time, RecA*-mediated LexA (both at the final concentration of 5.6 μM) proteolytic cleavage reactions conducted as stated above were stopped with 16 mM glutaraldehyde for 30 s before adding glycine to 60 mM (16).

Covalent cross-linking reactions: the LexA54 variant was reduced with 20 mM dithiothreitol (DTT) or oxidized with a mixture of 0.1 mM $CuSO_4$ and 0.5 mM 1,10-phenantroline for 30 min at room temperature. At the indicated time, RecA*-mediated proteolytic cleavage reactions of the oxidized LexA54 (at the final concentration of 4 and 5.6 μM for the LexA54 and RecA, respectively) conducted as stated above were stopped by adding 4xNuPAGE LDS sample buffer (Invitrogen). Presence of oxidant in the reactions did not affect RecA*-stimulated LexA self-cleavage, as determined by oxidation of wild-type LexA and implementation of self-cleavage reaction (data not shown).

Samples were analyzed as described above. We resolved the various repressor forms: dimers, monomers, CTDs, N-terminal domains (NTDs) and combinations of intact LexA protein and its cleavage products, by analysis of protein molar masses in comparison with the PageRuler prestained protein ladder (Fermentas) and by comparing our data with earlier results (16).

Spin labeling of LexA mutants

For spin labeling, purified single cysteine mutants (~10 mg) of *E. coli* LexA (Supplementary Table S2) were pretreated with DTT at 15 mM final concentration in buffer containing 20 mM NaH_2PO_4 (pH 7.3), 500 mM NaCl (4 h, 4°C). DTT was removed by exchanging the buffer two times with the use of PD-10 desalting column (GE Healthcare) and after removal protein solutions were incubated with 1 mM MTSSL (1-oxyl-2,2,5,5-tetramethyl-3-pyrroline-3-methyl) methanethiosulfonate spin label (Toronto Research, Alexis), for 16 h (8°C). Excess MTSSL was removed by exchanging the buffer two times with 20 mM NaH_2PO_4 (pH 7.3), 200 mM NaCl with a PD 10 desalting column. The spin-labeled proteins were concentrated to ~100 μM and buffer exchanged by buffer of the same composition containing deuterated water (Acros Organics) by the use of Amicon centrifugal filters (Millipore). Labeling efficiencies have been determined to be ~80% for LexA54 and >95% for LexA29 and LexA191.

EPR measurements

Distance measurements between nitroxide spin labels attached to the LexA variants (~100 μM) were carried out either unbound or bound to the 24 bp *tisB* operator-containing DNA fragment (5′-TTTACTGTAT AAATAAACAGTAAT-3′, marked are the SOS boxes) composed of oligonucleotide primers Tis_1b, Tis_2b (Supplementary Table S1). Cw EPR spectra for interspin distance determination in the range from ~0.8 to 2.0 nm were obtained on a homebuilt cw X-band EPR spectrometer equipped with a Super High Sensitivity Probehead (Bruker Biospin GmbH, Rheinstetten, Germany). The magnetic field was measured with a B-NM 12 B-field meter (Bruker Biospin). A continuous flow cryostat Oxford ESR9 (Oxford Instruments, Oxfordshire, UK) was used in combination with an Intelligent Temperature Controller (ITC 4; Oxford Instruments) to stabilize the sample temperature to 160 K. The microwave power was

set to 0.2 mW and the B-field modulation amplitude to 0.25 mT. EPR quartz capillaries (3 mm inner diameter) were filled with sample volumes of 40 μl. Fitting of simulated dipolar broadened EPR powder spectra to the experimental ones was carried out using the program *WinDipFit* (24).

Double electron–electron resonance (DEER)/PELDOR EPR experiments were performed at X-band frequencies (9.3–9.4 GHz) on a Bruker Elexsys 580 spectrometer equipped with a Bruker Flexline split-ring resonator ER 4118X-MS3. Temperature was stabilized to 50 K using a continuous flow helium cryostat (ESR900; Oxford Instruments) controlled by an Oxford Intelligent Temperature Controller ITC 503 S. EPR quartz capillaries (2.4 mm inner diameter) were filled with sample volumes of 40 μl.

All measurements were performed using the four-pulse DEER sequence with two microwave frequencies: $\pi/2(\upsilon_{obs}) - \tau_1 - \pi (\upsilon_{obs}) - t' - \pi (\upsilon_{pump}) - (\tau_1 + \tau_2 - t') - \pi (\upsilon_{obs}) - \tau_2 - $ echo (25,26). A two-step phase cycling $(+\langle x \rangle, - \langle x \rangle)$ was performed on $\pi/2(\upsilon_{obs})$. Time t' is varied, whereas τ_1 and τ_2 are kept constant. The dipolar evolution time is given by $t = t' - \tau_1$. Data were analyzed only for $t > 0$. The resonator was overcoupled and the pump frequency υ_{pump} was set to the center of the resonator dip (coinciding with the maximum of the nitroxide EPR spectrum) whereas the observer frequency υ_{obs} was 65 MHz higher (low-field local maximum of the spectrum). All measurements were performed at a temperature of 50 K with observer pulse lengths of 16 ns for $\pi/2$ and 32 ns for π pulses and a pump pulse length of 12 ns. Proton modulation was averaged by adding traces at eight different τ_1 values, starting at $\tau_{1,0} = 200$ ns and incrementing by $\Delta\tau_1 = 8$ ns. For proteins in D_2O buffer with deuterated glycerol, used for its effect on the phase relaxation, corresponding values were $\tau_{1,0} = 400$ ns and $\Delta\tau_1 = 56$ ns. Data points were collected in 8 ns time steps or, if the absence of fractions in the distance distribution below an appropriate threshold was checked experimentally, in 16 ns time steps. The total measurement time for each sample was 4–24 h. Analysis of the data was performed with DeerAnalysis 2009 (27).

Rotamer library analysis

The canonical ensemble of spin label side-chain (R1) conformations is modeled by a discrete set of 210 precalculated rotamers (28). From the rotamer library analysis, a conformational distribution of R1 at a specific position in the otherwise fixed protein structure can be determined. Briefly, the superposition of R1's backbone atoms onto the protein backbone at the respective position provides the orientation of R1 with respect to the protein structure. The resulting energy for the R1–protein interaction is then calculated from the Lennard Jones potential using the MD force field CHARMM27 (29). Subsequent Boltzmann weighting and normalization by the partition function gives a probability for each rotamer which is then multiplied by the probability of R1 to exhibit this conformation, resulting in the final rotamer probability distribution at the site of interest.

Between two such probability distributions a distance distribution is calculated as the histogram of all pairwise interspin distances weighted by the product of their respective probabilities. Structural aspects of LexA were generated using VMD software (30).

Functional properties Of LexA mutants

For EPR analysis, we selected LexA residues that are surface exposed and do not impair repressor functions when modified (31). *Esherichia coli* strain DM936 (*lexA41*) was transformed with plasmid pLexA29, pLexA54, pLexA191 to complement the temperature-sensitive LexA mutation. As a control strain DM936 expressing the wild-type *lexA* (pAna1) or expressing the repressor OxyR (pOxyR) was used. To verify the *in vivo* ability of the LexA mutants to regulate the SOS system and to repress the *sulA* gene, preventing induction of filamentous growth, strains were grown in Luria–Bertani (LB) ampicillin (Ap, 100 μg/ml) media at 28.0°C or at 42.5°C and in stationary phase cell counts were determined (20). Surface plasmon resonance (SPR) analysis and RecA*–mediated cleavage experiments were conducted as described in this chapter.

SPR assays

SPR RecA*–LexA interaction measurements were performed on a Biacore X (GE Healthcare) at 25°C. The streptavidin sensor chip was equilibrated with SPR_2 buffer containing 20 mM NaH_2PO_4 (pH 7.4), 150 mM NaCl, 2 mM $MgCl_2$, 1 mM DTT, 1 mM ATP (Sigma–Aldrich), 0.005% surfactant P20 (GE Healthcare). Approximately 200 response units (RU) of 5'-biotinylated 30-mer (32) was immobilized on the flow cell 2. Subsequently, RecA protein (2.1 μM) was passed in the SPR_2 buffer at 2 μl/min to create RecA*. The LexA119 repressor variant interacting with the 24 bp *tisB* operator (annealed primers Tis_1b, Tis_2b, Supplementary Table S1) or the 24-bp non-specific DNA (annealed primers Tis_1nb, Tis_2nb), free LexA119 or the DNA fragments, were injected across the immobilized RecA* (1000 RU) at 10 μl/min for 60 s, to study the interaction. The sensor chip with bound RecA* was regenerated by injection of 500 mM NaCl. A 0.05% SDS was used to additionally regenerate flow cell 1.

SPR LexA–operator interaction measurements were performed on a Biacore T100 at 25°C. The 88 bp *recA*, 114 bp *tisB*, 121 bp *cka* operator-containing DNA fragments and the *cka*-UP3 DNA fragment were PCR amplified and gel purified as described above. The resulting fragments were 5'-end biotinylated. The streptavidin sensor chip was equilibrated with SPR_1 buffer containing 20 mM Tris–HCl (pH 7.4), 150 mM NaCl, 0.005% surfactant P20 (GE Healthcare). The biotinylated DNA in SPR buffer was immobilized to approximately 20 RUs. An empty flow cell was used as a control. The interaction between LexA and chip-immobilized DNA was studied by injecting various concentrations of LexA or LexA71 in SPR buffer. The sensor chip with bound DNA was regenerated by injection of SPR buffer containing 500 mM NaCl. We noted that the interaction of both LexA and LexA71 with DNA was extremely rapid and

use of standard assays revealed that it is heavily influenced by the mass transfer effect (33). However, the dissociation of the proteins from the DNA was not influenced by the flow rate of the SPR buffer. For the final determination of dissociation rates, proteins were injected across the surface chip at a saturating concentration (40 nM) for 30 s and dissociation was followed for 20 min at a flow rate of 100 µl/min. The dissociation of LexA71 from *cka* operator was extremely slow; therefore, we followed dissociation for 40 min. The data were doubly referenced and fitted to a 1:1 binding model to obtain the dissociation rates constants. Three to six independent experiments were performed.

Persistence of *lexA* defective strain complemented by LexA and its variants

For the persistence assay, strain RW542 (*thr-1 araD139* Δ(*gpt-proA*)62 *lacY1 tsx-33 supE44 galK2 hisG4 rpsL31 xyl-5 mtl-1 argE3 thi-1 sulA211 lexA51*), encoding a defective LexA protein that cannot bind to target DNA sites due to impaired dimerization (18) was used. The λDE3 prophage, encoding the T7 RNA polymerase, was integrated into the RW542 chromosome according to instructions (λDE3 Lysogenization kit, Novagen). The λDE3 lysogenic RW542 strain, designated MB542, exhibited basal-level T7 RNA polymerase expression without addition of isopropyl beta-D-1-thiogalacto-pyranoside as determined according to the manufacturer's instructions. Subsequently, strain MB542 was transformed with plasmid harboring T7 promoter controlled wild-type *lexA*, mutant *lexA119* or the double-mutant *lexA71-119*. The minimum inhibitory concentration (MIC) for mitomycin C (Sigma) was determined by the broth dilution method (34). The MIC for the strain MB542 *lexA*(Def) was 3.2 µg/ml, for the strain harboring the plasmid encoding wild-type repressor 4.0 and 1.8 µg/ml for the strains with *lexA119* or the double *lexA71-119* mutant. The 2.5 MIC of mitomycin C was used for the persister assay. The isogenic strain RW118 expressing chromosomally encoded *lexA* exhibited identical mitomycin C MIC as the strain MB542 complemented with the plasmid encoding wild-type repressor. Thus, data indicate that the SOS system of the *lexA* complemented strain MB542 pAna1 functioned similarly as the wild-type strain. Experiments were conducted at 37°C essentially as described previously (35) except that transformed strains were grown (180 rpm) in 10 ml LB medium supplemented with 100 µg/ml Ap and cell counts determined by plating on LB or LBAp agar plates. No difference in cell count was detected when cells were plated on LB or LBAp media, indicating that plasmid loss did not occur during the experiments (data not shown). The percentage of survival was determined as the ratio of colony forming units (cfu) before to cfu following exposure to mitomycin C and plotted as a function of time.

Trypsin cleavage of LexA repressor bound to operator

The LexA repressor (2.4 µM) was bound to the *recA* or *cka* operator-containing fragments or to the *cka* variant fragments *cka*-UP1 or *cka*-UP3. The LexA dimer to operator/modified operator ratio was 1:2. DPPC-treated Trypsin (Sigma–Aldrich) digestions were conducted at 25°C in DNA-binding buffer at a LexA concentration of 2.4 µM with a protease to repressor ratio of 1:50 (m:m). The reaction time course was initiated with the addition of the protease. Bands were resolved as described above.

Western blotting

Thrombin (Novagen) digestion of 3.4 µM LexA was carried out at 20°C for 2 h in 20 mM Tris (pH 7.3), 200 mM NaCl with a protease to repressor weight ratio of 1:2000. LexA–DNA complex was formed by 10 min incubation of 3.4 µM LexA and DNA fragment-containing *recA* operator in the LexA dimer toward operator ratio 1:2 at 37°C in DNA-binding buffer prior to trypsin digestion carried out for 30 min as described above. Samples were resolved on a 12% acrylamide gel. Blotting and detection was done as described before (36). Primarily, the proteins were stained with mouse anti-hexa-histidine tag antibody (Quiagen) and secondary antibodies conjugated by horseradish peroxidase. The same membrane was re-stained by primary LexA rabbit poly-clonal antibody (Upstate) and same secondary antibodies. Antibodies were used at a concentration of 0.5 µg/ml.

Agarose gel mobility shift assays

The LexA repressor was, immediately before use, serially diluted from 2.4 µM to 2.0 nM. The 10 µl reaction mixtures contained ~50 mM *recA*, *tisB* or ~25 mM *cka* operator-containing DNA or its variants *cka*-UP1 or *cka*-UP3, interacting with LexA in the DNA-binding buffer. Protein–DNA complexes were resolved on 2.5% agarose gels (20) after incubation at room temperature for 10 min in 20 mM Tris (pH 7.5), 200 mM NaCl, 1 mM EDTA, 12% glycerol.

RESULTS AND DISCUSSION

DNA is an allosteric effector of bacterial LexA protein

It was previously suggested that SOS box-containing DNA fragments can inhibit RecA*-mediated LexA self-cleavage (37). In contrast, recently published LexA–DNA crystal structures indicate that LexA–operator interaction exerts minimal interference with RecA*-induced self-cleavage (38).

Most of the *E. coli* SOS genes possess a single SOS box, but the number of operators can range up to 3 (7). We have measured rates of RecA*-stimulated self-inactivation of purified LexA interacting with either tandem (colicin K gene, *cka*) or modified, lower LexA affinity tandem operator (*cka*-UP1) or single (*recA*) operator-containing DNA fragment in comparison with the non-specific DNA (*cka*-UP3) (Supplementary Figures S1 and S2). The results shown in Figure 1A–E indicate that RecA* cannot induce self-cleavage in LexA that is bound to target DNA operator sites. This was confirmed by measuring LexA inactivation in reactions with a range of concentrations of specific (*cka* operators) or non-specific DNA. Non-specific DNA had little inhibitory effect on LexA

induced inactivation, in comparison with the operator-containing DNA (Figure 1F and G).

It has been suggested that it is not possible for both subunits of a LexA dimer to simultaneously make contact with the deep helical groove of RecA*, and that separate docking events are required to cleave both LexA subunits (38). Thus, we used glutaraldehyde cross-linking to follow the kinetics of RecA*-mediated cleavage of unbound LexA repressor and found that self-cleavage proceeds primarily via one subunit of a dimer (Figure 2A). The reaction reached completion by 20 min (Supplementary Figure S3). Data indicate that RecA* predominately induces self-cleavage in one monomer of the LexA dimer and that the resulting LexA–LexA/CTD heterodimer is an inactive intermediate, exhibiting weaker DNA binding (31).

The LexA repressor is mostly dimeric at the concentration used for the glutaraldehyde cross-linking experiment (4); however, complete cross-linking of the dimers could not be achieved. Thus, a cysteine cross-linking experiment was expl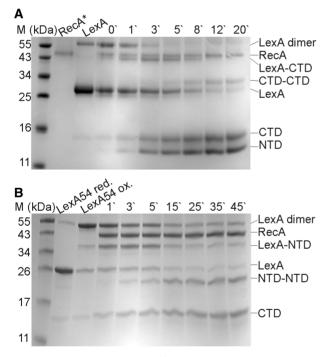oited. Structural data of the unbound LexA dimer suggest that residues Gly54 positioned in the DNA-binding NTDs could come in close proximity (13). Data show that the oxidized repressor derivative LexA54, with Gly 54 replaced by Cys, forms covalently bound dimers (Figure 2B). Hence, to complement the glutaraldehyde cross-linking data, RecA*-induced self-cleavage of oxidized LexA54 was determined. The kinetics of appearance of a singly cleaved LexA dimer in the time course of the cleavage reaction indicate that, the LexA heterodimer is an intermediate on the pathway that leads to the fully cleaved dimer (Figure 2). Thus, two successive dockings with RecA* are necessary for the inactivation of both repressor subunits.

Intracellularly, almost all LexA is dimeric (4) and pre-existing repressors dissociate slowly to monomers (16). Thus, the source of monomers is supposedly newly synthesized LexA. We propose that, following DNA damage repair and disappearance of the SOS-inducing signal, both newly synthesized LexA as well as heterodimers could provide a source of monomers for resetting repression and for fine-tuning of the SOS response.

LexA conformational dynamics

A recent report of the structure of LexA–operator complexes suggested that flexibility in bound LexA could facilitate interaction with RecA*, leading to LexA self-cleavage, provoking separation of the DNA-binding domain from the rest of the operator–bound dimer and inactivation (38). To test this directly, we used site-directed spin labeling EPR (39) in combination with DEER (25,26) spectroscopy. Interactions between the paramagnetic centers attached to the two subunits of the LexA dimer were measured in order to investigate the mobility of both the N-terminal DNA-binding domain and the C-terminal, regulatory domain, in free and DNA-bound LexA. LexA derivatives with single cysteines substituting residues Ala29 or Gly54 in the DNA-binding domain or residue Leu191 in the dimerization domain were spin labeled (Figure 3A and B, Supplementary Table S2 and Figure S4).

Measurements of the interaction between the spin-label side chains (denoted R1) reveal high-conformational flexibility of the DNA-binding domains in the unbound repressor (apo), but a defined conformation when bound to a specific DNA target. For spin labels at positions 29 (A29R1) or 54 (G54R1) in the apo state broad, multi-modal interspin distance distributions are revealed ranging from 30 to 65 Å and from 15 to 50 Å, respectively (Figure 3C, solid lines, inset and Supplementary Figures S5 and S6). Remarkably, for A29R1 and G54R1 in the apo state the DEER traces (Supplementary Figure S5) exhibit significantly smaller modulation depths, compared with the DNA bound state. For A29R1, this observation can be explained by the presence of a significant fraction of the protein molecules with interspin distances beyond the range accessible to DEER experiments (>70 Å). For G54R1, the reduced modulation depth in the apo state is caused by the contributions of molecules with interspin distances <15 Å which do not contribute to the DEER signal as revealed by cw EPR data. Thus, high
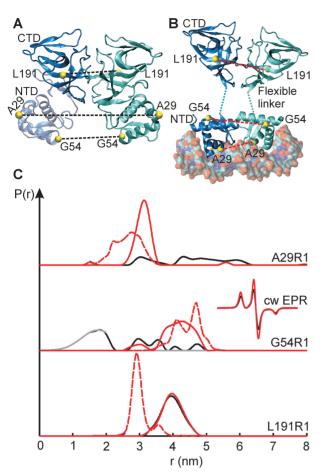

Figure 2. RecA*-induced LexA self-cleavage proceeds primarily by one subunit. (**A**) Cleavage of unbound LexA was induced by addition of RecA*, and samples were cross-linked by glutaraldehyde at different time points (min) and analyzed by gel electrophoresis. RecA and LexA markers were also cross-linked as indicated. Homodimer (LexA dimer), LexA monomer cross-linked to the C-terminal fragment (LexA–CTD), cross-linked C-terminal fragments (CTD–CTD), monomer (LexA) and cleavage forms of LexA (CTD, NTD) are marked. (**B**) The LexA54 derivate with residue Gly54 replaced by Cys in the DNA-binding domain was reduced (LexA54 red.) or oxidized (LexA54 ox.) to show that the repressor can be covalently bound at residue 54. Cleavage of oxidized LexA54 was induced by addition of RecA* and samples taken at different time points (min) and analyzed by SDS–PAGE electrophoresis. Homodimer (LexA dimer), LexA monomer cross-linked to the N-terminal fragment (LexA–NTD), monomer (LexA), cross-linked N-terminal fragments (NTD–NTD), and C-terminal fragment (CTD) are marked.

Figure 3. Conformational dynamics of the LexA binding to the *tisB* operator. (**A**) Structure of unbound LexA dimer [pdb ID:1JHH (13)] with modeled (20) undetermined residues (transparent) and (**B**), operator-bound LexA [pdb ID:3JSO (38)]. Individual subunits are colored blue and cyan, residues changed to cysteines and spin labeled are presented as yellow beads. Interspin distances were determined for spin-label pairs connected by dashed lines. (**C**) Experimental interspin distance distributions measured by DEER (solid lines) and simulations based on LexA crystal structures (dashed lines) for the DNA bound (red) and apo states (black). For G54R1 in the apo state, the distribution for interspin distances <2 nm (gray) was determined from the dipolar broadened cw EPR spectra (Supplementary Data). Results are shown as normalized probability distributions.

flexibility of the DNA-binding domains is obvious as they sample conformations leading to interspin distances ranging from 25 to >70 Å for A29R1 and <15 to 50 Å for G54R1. In contrast, in the operator-bound state both mutants show single population maxima centered at 31 Å (± 3 Å) for A29R1, and at 43 Å (± 5 Å) for G54R1. Remarkably, the distance distributions of both constructs indicate that the conformations LexA samples in the apo state cover also the DNA bound structure. Measurements with labeled LexA191 (L191R1) revealed that interspin distance distributions were very similar in both the unbound and DNA bound states, with a clear maximum at a distance of 40 Å (Figure 3C). Hence, the C-terminal regulatory domains of each subunit in the LexA dimer function as a rigid scaffold for the DNA-binding NTDs. In the unbound state, these are flexible and can adapt the conformation in which the RecA*-induced attack of the

scissile A84–G85 bond by the active-site Ser119 is facilitated. On the contrary, in the rigid operator-bound state of the LexA dimer, this conformation cannot be accessed and RecA*-induced inactivation of LexA is prevented.

Again, an interesting observation concerns the modulation depths of the DEER traces, which is significantly lower for A29R1 and G54R1 in the NTDs compared with L191R1 in the CTD (Supplementary Figure S5). Although a lower labeling efficiency of ~80% has been obtained for G54R1 (A29R1 and L191R1: >95%), this does not explain the observed differences in the modulation depths. Instead, this observation is in line with the fact that unbound LexA has been shown to undergo the process of self-cleavage (13), leading to LexA–LexA/CTD heterodimer formation. Such heterodimers contain two spin labels in the CTD, but only one spin-labeled NTD is present, thus explaining the lower modulation depth for A29R1 and G54R1.

A comparison of the experimental interspin distances for LexA-A29R1, G54R1 and L191R1 in the DNA bound state with values predicted from the LexA–DNA crystal structure (pdb ID:3JSO) using the rotamer library approach (Figure 3C, dashed lines) shows reasonable agreement for the two positions located in the NTDs (A29R1 and G54R1) indicating that, the arrangement found in the crystal structures seems to reflect the state in solution well. On the contrary, the data for L191R1 indicate that the conformation of the LexA dimerization domain in solution might slightly differ from that observed in crystals, most probably due to crystal packing effects. Nevertheless, it cannot be excluded that limitations in the accuracy of the rotamer library approach account for the observed differences.

Repressor's dissociation from operators orchestrates SOS response

SPR analysis was subsequently performed to determine the mechanism of operator-bound repressor interference with RecA*-induced autoproteolysis. Active RecA filament was formed on single-stranded DNA bound to the surface of the sensor chip (Figure 4A). Non-cleavable repressor variant LexA119 (S119A) interacted with chip-immobilized RecA* in a concentration-dependent manner (Figure 4B). The presence of *tisB* operator interfered with the ability of LexA119 to bind to RecA* (Figure 4C). We show that binding of operator induces LexA in a particular conformation in which interaction with RecA* is precluded (Figure 4D), revealing why RecA*-induced inactivation of specifically bound LexA is unfeasible.

The LexA CTD provides the determinants for dimerization and self-cleavage activity, thus the interface interacting with RecA* (13). In the crystal structure of the unbound LexA mutant dimer (pdb ID: 1JHH) one subunit is well ordered throughout and in a non-cleavable state, whereas the second subunit, while disordered in the NTD, adopts the cleavable state in the CTD (13). The structure of the intact monomer also exhibits LexA intramolecular contacts between the DNA-binding NTD and
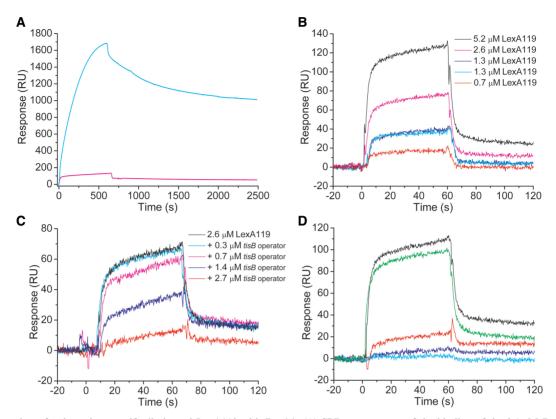
Figure 4. Interaction of unbound or specifically bound LexA119 with RecA*. (**A**) SPR sensorgrams of the binding of the 2.1 μM RecA to the flow cell 1 (red) or to the flow cell 2 with immobilized *tisB*-operator DNA (cyan). (**B**) Unbound LexA119 repressor in concentration range from 0.7 to 5.2 μM or (**C**) LexA119 interacting with 24-bp *tisB* operator DNA in concentration range from 0.3 to 2.7 μM were injected across the chip-immobilized RecA* for 60 s at 10 μl/min. The used DNA to repressor ratio (mol:mol) was approximately 0.1:1, 0.3:1, 0.5:1, 1:1, 2:1, respectively. (**D**) Sensorgrams of the 2.6 μM repressor variant LexA119 (black), the 24 bp DNA fragments (2.7 μM) consisting of the *tisB* operator (violet) or the non-specific DNA (cyan), *tisB* operator bound LexA119 (red) or LexA119 mixed with the non-specific DNA (green), interacting with the chip-immobilized RecA*. The used DNA to repressor ratio was ∼2:1 (mol:mol).

the cleavage site loop lying just within the CTD. This is most likely not an artifact due to crystal packing (13) as cleavage site region–NTD interactions were also confirmed by experiments exploiting cysteine cross-linking (20). Thus, orientation of NTDs might affect the position of the cleavage loop containing the scissile peptide bond. Our EPR results indicate that a five residue hydrophilic linker that connects the NTD of LexA to its catalytic core domain does not impede movement of the NTDs, as suggested previously (20). Thus, although LexA is a homodimeric protein, variable positions of its NTDs in the dimer might modulate the position of the cleavage-site regions in the CTDs.

The repressor recognizes its targets as a dimer (4) and the dimer does not exert stringency requirement on the binding domain (38). In the operator-bound LexA, an extensive dimer interface is observed between the DNA-binding NTDs, formed of residues which are solvent exposed in the unbound LexA (13). Interactions between the two DNA-binding domains are acting synergistic with DNA binding, thus increasing LexA dimer stability by 1000-fold (4,38). In contrast to the alternating conformations of the cleavage loops in the unbound LexA dimers, both scissile peptide bonds in the operator-bound mutant dimers are displaced or docked

in the active center (38). The results of this investigation show that the operator is an alosteric effector of the LexA repressor indicating that, a specific orientation of the DNA-binding NTDs sets the repressor in a conformation in which interaction with RecA* and a subsequent self-cleavage reaction is precluded. Interestingly, mutations in LexA that specifically impair RecA*-dependent cleavage, but do not alter catalysis have not been identified (16). Therefore, further studies will be employed to elucidate how diverse positions of the LexA cleavage loop and orientation of the NTDs modulate interaction with the RecA*.

Our results imply that LexA dissociation from operators coordinates expression of the SOS genes. This is in agreement with previous reports, showing that the timing of induction of LexA-regulated genes correlates with the binding affinity of the SOS boxes (1). However, previously LexA operator affinity was ranked by quantitative gel retardation and DNase I footprinting experiments and by calculating the relatedness of an operator sequence to that of the consensus sequence derived from the known LexA targets (18,23). To provide further details, we used SPR to measure LexA–operator interactions under near physiological salt and pH conditions in real time. We used DNA fragments that contained *recA*, *tisB*, *cka* operators

or non-specific DNA *cka*-UP3. Binding to operators was concentration dependent (data not shown), but LexA did not bind to the control DNA (Figure 5). The association of LexA with the SOS operators was extremely rapid, and it was therefore not possible to determine accurately the association rate constants due to the mass transfer effect. Control experiments showed that dissociation of LexA from the surface of the chip was not dependent on the flow rate (data not shown), therefore it was possible to determine the rates of dissociation. In spite of rapid LexA association with all the tested operators, the repressor exhibited diverse dissociation rates. Dissociation was similar for *recA* and *tisB*, but significantly slower from the *cka* operator. This explains, for example, why *recA* is one of the first transcribed genes in the SOS response, while expression of the *cka* gene is delayed, limited to conditions of extensive, long-lived DNA damage (1,11). We conclude that differences between LexA operators affect repressor dissociation and influence the timing of expression of SOS genes.

Decreasing persister formation by modulating LexA functions

The insights into LexA functions presented here may provide new directions in the battle against the emergence and spread of drug resistance. It has recently been shown that persisters form during the SOS response and depend on the LexA-regulated TisB toxin (40). Hence, bacterial killing by antibiotics can be enhanced by dislabeling the

SOS response, either by deleting the *recA* gene (41) or overexpression of non-cleavable *lexA* variants (42,43). We used the LexA71 (E71K) repressor variant (21) that exhibits three to nine times slower dissociation from operators compared with wild-type LexA repressor (Figure 5). We then measured persister formation in an *E. coli* strain defective for *lexA*, complemented with wild-type LexA or its non-cleavable mutants, exhibiting either normal or enhanced DNA binding, treated with 2.5 times MIC of mitomycin C. Our results (Figure 6) show that the occurrence of persister cells in bacterial populations triggered by DNA damage can be altered by changing LexA activity. Notably, when cells expressed the non-cleavable and enhanced operator-binding LexA repressor variant, no persisters were detected 1 h after induced DNA damage. LexA homologs are found in prokaryotes (31), but to date there are no known orthologs in eukaryotes. Hence, this work sets a novel platform for drug discovery to treat bacterial pathogens and offers an approach to control bacterial survival of antibiotic therapy.

CONCLUSIONS

In the present paper, we show that RecA*-mediated LexA repressor self-cleavage cannot be induced in LexA specifically bound to target DNA. Our results contradict the observation that the LexA operator bound conformation allows docking to RecA* and subsequent LexA
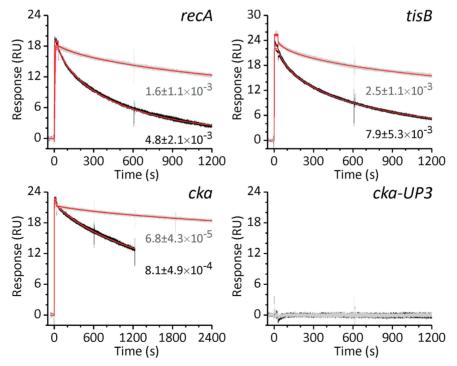

Figure 5. Interaction of LexA and LexA71 with various promoter regions. SPR was used to assess the interaction of LexA (black) or LexA71 (gray) with various operators as indicated. Biotinylated DNA fragments were immobilized on the surface of the streptavidin sensor chip. Purified protein at saturating concentration was injected across the chip for 30 s and dissociation followed as shown on the graphs. The sensorgrams were doubly referenced and fitted to a 1:1 binding model. Data shown are triplicate injections of the protein and overlaid with fits (red). Calculated dissociation rate constants (average ± standard deviation) are shown for each condition.
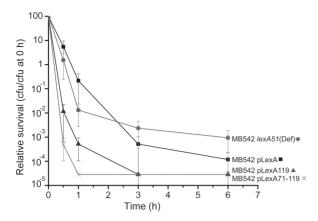
Figure 6. Mitomycin C survival of the *E. coli lexA⁻* strain complemented with LexA repressor variants. MB542 (*lexA51*) strain complemented with wild-type LexA (pLexA) or its non-cleavable mutants exhibiting either normal (pLexA119) or enhanced DNA (pLexA71–119) binding was grown to exponential phase (~10^8 cfu/ml), when exposed to 2.5 times MIC of mitomycin C. At 0, 0.5, 1, 3, 6 h after addition, viable cell number was determined (cfu/ml). As a control, strain MB542 was used. The data points are averages of at least four independent experiments and error bars indicate the standard error.

inactivation (38). Thus, diverse LexA conformations enable either repression of SOS genes by specific DNA binding or repressor cleavage in response to DNA damage. Data presented here imply that mobility of the LexA NTDs affects the repressor's interaction with the RecA*. Our results indicate that RecA*-mediated inactivation of unbound LexA must decrease the intracellular pool of free LexA which provokes dissociation of the functional repressor from its DNA targets (Figure 7). Taken together, our results indicate how the signal from DNA damage at a particular chromosomal location is transduced into the induction of the SOS genes, co-ordinated by the distinct LexA repressor conformations. In addition, we show that, upon DNA damage, separate interactions between the two key SOS players are required to cleave both subunits of the LexA dimer. Therefore, when the inducing signal disappears, the remaining self-cleavage intermediates, inactive heterodimers, can provide a source of subunits which dimerize into the functional repressor to accelerate resetting of the system.
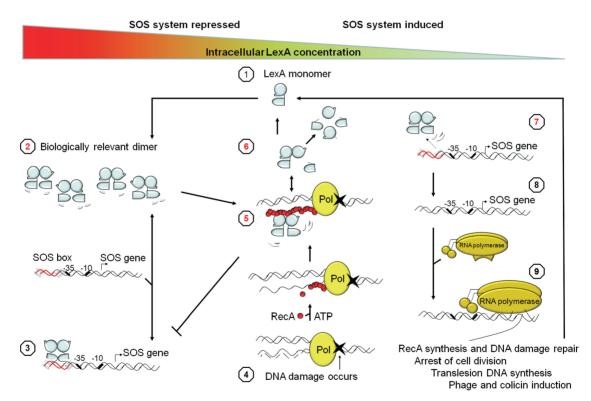

Figure 7. An overview of the SOS response in *E. coli.* (1) Concentration of LexA monomers increases. (2) LexA monomers in solution form biologically relevant dimers. DNA-binding domains of the unbound LexA are highly mobile and can move freely to one another. (3) Repression of the SOS system occurs when LexA dimers bind specifically to SOS boxes located at the promoter regions of SOS genes and sterically precludes their transcription. (4) The polymerase III holoenzyme (Pol) carries out DNA replication. At the site of DNA damage PolIII arrests, and single-stranded DNA (ssDNA) accumulates. RecA binds to ssDNA in the presence of ATP, forming active RecA–ssDNA–ATP filaments (RecA*). (5) RecA* induces self-cleavage in the unbound LexA but cannot stimulate inactivation of LexA specifically bound to target DNA. (6) In the unbound repressor dimer, one monomer is preferentially inactivated and the uncleaved monomer could affect resetting of the system. Cleaved LexA products are rapidly degraded by the ClpXP and Lon proteases (44). (7) Due to induced unbound LexA self-cleavage, intracellular LexA pool decreases. Specifically bound LexA repressor dissociates from operators, (8) leading to co-ordinated de-repression of SOS genes. (9) The rate of LexA dissociation from target sites is influenced by operator sequences and acts in orchestrating the response. Subsequently, as DNA damage is repaired, SOS induction is reversed. Numbers in red indicate novel insights into the system.

SUPPLEMENTARY DATA

Supplementary Data are available at NAR Online.

FUNDING

Conflict of interest statement. None declared.

REFERENCES

1. Courcelle,J., Khodursky,A., Peter,B., Brown,P.O. and Hanawalt,P.C. (2001) Comparative gene expression profiles following UV exposure in wild-type and SOS-deficient Escherichia coli. *Genetics*, **158**, 41–64.
2. Wade,J.T., Reppas,N.B., Church,G.M. and Struhl,K. (2005) Genomic analysis of LexA binding reveals the permissive nature of the Escherichia coli genome and identifies unconventional target sites. *Genes Dev.*, **19**, 2619–2630.
3. Sassanfar,M. and Roberts,J.W. (1990) Nature of the SOS-inducing signal in Escherichia coli. The involvement of DNA replication. *J. Mol. Biol.*, **212**, 79–96.
4. Mohana-Borges,R., Pacheco,A.B., Sousa,F.J., Foguel,D., Almeida,D.F. and Silva,J.L. (2000) LexA repressor forms stable dimers in solution. The role of specific dna in tightening protein-protein interactions. *J. Biol. Chem.*, **275**, 4708–4712.
5. Gowers,D.M. and Halford,S.E. (2003) Protein motion from non-specific to specific DNA by three-dimensional routes aided by supercoiling. *EMBO J.*, **22**, 1410–1418.
6. Blainey,P.C., Luo,G., Kou,S.C., Mangel,W.F., Verdine,G.L., Bagchi,B. and Xie,X.S. (2009) Nonspecifically bound proteins spin while diffusing along DNA. *Nat. Struct. Mol. Biol.*, **16**, 1224–1229.
7. Keseler,I.M., Bonavides-Martinez,C., Collado-Vides,J., Gama-Castro,S., Gunsalus,R.P., Johnson,D.A., Krummenacker,M., Nolan,L.M., Paley,S., Paulsen,I.T. *et al.* (2009) EcoCyc: a comprehensive view of Escherichia coli biology. *Nucleic Acids Res.*, **37**, D464–470.
8. Little,J.W. (1991) Mechanism of specific LexA cleavage: autodigestion and the role of RecA coprotease. *Biochimie*, **73**, 411–421.
9. Neher,S.B., Flynn,J.M., Sauer,R.T. and Baker,T.A. (2003) Latent ClpX-recognition signals ensure LexA destruction after DNA damage. *Genes Dev.*, **17**, 1084–1089.
10. Napolitano,R., Janel-Bintz,R., Wagner,J. and Fuchs,R.P. (2000) All three SOS-inducible DNA polymerases (Pol II, Pol IV and Pol V) are involved in induced mutagenesis. *Embo J.*, **19**, 6259–6265.
11. Cascales,E., Buchanan,S.K., Duche,D., Kleanthous,C., Lloubes,R., Postle,K., Riley,M., Slatin,S. and Cavard,D. (2007) Colicin biology. *Microbiol. Mol. Biol. Rev.*, **71**, 158–229.
12. Galkin,V.E., Yu,X., Bielnicki,J., Ndjonka,D., Bell,C.E. and Egelman,E.H. (2009) Cleavage of bacteriophage lambda cI repressor involves the RecA C-terminal domain. *J. Mol. Biol.*, **385**, 779–787.
13. Luo,Y., Pfuetzner,R.A., Mosimann,S., Paetzel,M., Frey,E.A., Cherney,M., Kim,B., Little,J.W. and Strynadka,N.C. (2001) Crystal structure of LexA: a conformational switch for regulation of self-cleavage. *Cell*, **106**, 585–594.
14. Cohen,S., Knoll,B.J., Little,J.W. and Mount,D.W. (1981) Preferential cleavage of phage lambda repressor monomers by recA protease. *Nature*, **294**, 182–184.
15. Pawlowski,D.R. and Koudelka,G.B. (2004) The preferred substrate for RecA-mediated cleavage of bacteriophage 434 repressor is the DNA-bound dimer. *J. Bacteriol.*, **186**, 1–7.
16. Giese,K.C., Michalowski,C.B. and Little,J.W. (2008) RecA-dependent cleavage of LexA dimers. *J. Mol. Biol.*, **377**, 148–161.
17. Mustard,J.A. and Little,J.W. (2000) Analysis of Escherichia coli RecA interactions with LexA, lambda CI, and UmuD by site-directed mutagenesis of recA. *J. Bacteriol.*, **182**, 1659–1670.
18. Fernandez De Henestrosa,A.R., Ogi,T., Aoyagi,S., Chafin,D., Hayes,J.J., Ohmori,H. and Woodgate,R. (2000) Identification of additional genes belonging to the LexA regulon in Escherichia coli. *Mol. Microbiol.*, **35**, 1560–1572.
19. Kristan,K., Viero,G., Macek,P., Dalla Serra,M. and Anderluh,G. (2007) The equinatoxin N-terminus is transferred across planar lipid membranes and helps to stabilize the transmembrane pore. *FEBS J.*, **274**, 539–550.
20. Butala,M., Hodoscek,M., Anderluh,G., Podlesek,Z. and Zgur-Bertok,D. (2007) Intradomain LexA rotation is a prerequisite for DNA binding specificity. *FEBS Lett.*, **581**, 4816–4820.
21. Oertel-Buchheit,P., Porte,D., Schnarr,M. and Granger-Schnarr,M. (1992) Isolation and characterization of LexA mutant repressors with enhanced DNA binding affinity. *J. Mol. Biol.*, **225**, 609–620.
22. Mrak,P., Podlesek,Z., van Putten,J.P. and Zgur-Bertok,D. (2007) Heterogeneity in expression of the Escherichia coli colicin K activity gene cka is controlled by the SOS system and stochastic factors. *Mol. Genet. Genomics*, **277**, 391–401.
23. Lewis,L.K., Harlow,G.R., Gregg-Jolly,L.A. and Mount,D.W. (1994) Identification of high affinity binding sites for LexA which define new DNA damage-inducible genes in Escherichia coli. *J. Mol. Biol.*, **241**, 507–523.
24. Steinhoff,H.J., Radzwill,N., Thevis,W., Lenz,V., Brandenburg,D., Antson,A., Dodson,G. and Wollmer,A. (1997) Determination of interspin distances between spin labels attached to insulin: comparison of electron paramagnetic resonance data with the X-ray structure. *Biophys. J.*, **73**, 3287–3298.
25. Martin,R.E., Pannier,M., Diederich,F., Gramlich,V., Hubrich,M. and Spiess,H.W. (1998) Determination of end-to-end distances in a series of TEMPO diradicals of up to 2.8 nm length with a new four-pulse double electron electron resonance experiment. *Angew. Chem. Int. Edit.*, **37**, 2834–2837.
26. Pannier,M., Veit,S., Godt,A., Jeschke,G. and Spiess,H.W. (2000) Dead-time free measurement of dipole-dipole interactions between electron spins. *J. Magn. Reson.*, **142**, 331–340.
27. Jeschke,G., Chechik,V., Ionita,P., Godt,A., Zimmermann,H., Banham,J., Timmel,C.R., Hilger,D. and Jung,H. (2006) DeerAnalysis2006 - a comprehensive software package for analyzing pulsed ELDOR data. *Appl. Magn. Reson.*, **30**, 473–498.
28. Polyhach,Y., Bordignon,E. and Jeschke,G. (2011) Rotamer libraries of spin labelled cysteines for protein studies. *Phys. Chem. Chem. Phys.*, **13**, 2356–2366.
29. Mackerell,A.D. Jr., Feig,M. and Brooks,C.L. 3rd (2004) Extending the treatment of backbone energetics in protein force fields: limitations of gas-phase quantum mechanics in reproducing protein conformational distributions in molecular dynamics simulations. *J. Comput. Chem.*, **25**, 1400–1415.
30. Humphrey,W., Dalke,A. and Schulten,K. (1996) VMD: visual molecular dynamics. *J. Mol. Graph.*, **14**, 33–38, 27–38.
31. Butala,M., Zgur-Bertok,D. and Busby,S.J. (2009) The bacterial LexA transcriptional repressor. *Cell Mol. Life Sci.*, **66**, 82–93.
32. Jiang,Q., Karata,K., Woodgate,R., Cox,M.M. and Goodman,M.F. (2009) The active form of DNA polymerase V is UmuD'(2)C-RecA-ATP. *Nature*, **460**, 359–363.
33. Rich,R.L. and Myszka,D.G. (2010) Grading the commercial optical biosensor literature-Class of 2008: 'The Mighty Binders'. *J. Mol. Recognit.*, **23**, 1–64.
34. Miller,J.H. (1972) *Experiments in Molecular Genetics.* Cold Spring Harbor Press, Cold Spring Harbor, New York, USA.
35. Dorr,T., Lewis,K. and Vulic,M. (2009) SOS response induces persistence to fluoroquinolones in Escherichia coli. *PLoS Genet.*, **5**, e1000760.
36. Kristan,K., Podlesek,Z., Hojnik,V., Gutierrez-Aguirre,I., Guncar,G., Turk,D., Gonzalez-Manas,J.M., Lakey,J.H., Macek,P. and Anderluh,G. (2004) Pore formation by equinatoxin, a eukaryotic pore-forming toxin, requires a flexible N-terminal region and a stable beta-sandwich. *J. Biol. Chem.*, **279**, 46509–46517.

37. Little,J.W. and Mount,D.W. (1982) The SOS regulatory system of Escherichia coli. *Cell*, **29**, 11–22.

38. Zhang,A.P., Pigli,Y.Z. and Rice,P.A. (2010) Structure of the LexA-DNA complex and implications for SOS box measurement. *Nature*, **466**, 883–886.

39. Klare,J.P. and Steinhoff,H.J. (2009) Spin labeling EPR. *Photosynth. Res.*, **102**, 377–390.

40. Dorr,T., Vulic,M. and Lewis,K. (2010) Ciprofloxacin causes persister formation by inducing the TisB toxin in Escherichia coli. *PLoS Biol.*, **8**, e1000317.

41. Kohanski,M.A., Dwyer,D.J., Hayete,B., Lawrence,C.A. and Collins,J.J. (2007) A common mechanism of cellular death induced by bactericidal antibiotics. *Cell*, **130**, 797–810.

42. Cirz,R.T., Chin,J.K., Andes,D.R., de Crecy-Lagard,V., Craig,W.A. and Romesberg,F.E. (2005) Inhibition of mutation and combating the evolution of antibiotic resistance. *PLoS Biol.*, **3**, e176.

43. Lu,T.K. and Collins,J.J. (2009) Engineered bacteriophage targeting gene networks as adjuvants for antibiotic therapy. *Proc. Natl Acad. Sci. USA*, **106**, 4629–4634.

44. Pruteanu,M. and Baker,T.A. (2009) Proteolysis in the SOS response and metal homeostasis in Escherichia coli. *Res. Microbiol.*, **160**, 677–683.